IEEE Access
Multidisciplinary | Rapid Review | Open Access Journal

Received May 31, 2018, accepted June 26, 2018, date of publication July 5, 2018, date of current version August 7, 2018.

Digital Object Identifier 10.1109/ACCESS.2018.2853164

An Improved Method for Accurate Extraction of Coupling Coefficient Between a Lossy Radiator and a Lossless Resonator in Filtering Antennas

QIONG-SEN WU[1,2], (Member, IEEE), XIAO ZHANG[2,3], (Member, IEEE), AND LEI ZHU[2], (Fellow, IEEE)

[1]School of Information Engineering, Guangdong University of Technology, Guangzhou 510006, China
[2]Department of Electrical and Computer Engineering, Faculty of Science and Technology, University of Macau, Macau, China
[3]ATR National Key Laboratory of Defense Technology, College of Information Engineering, Shenzhen University, Shenzhen 518060, China

Corresponding author: Lei Zhu (leizhu@umac.mo)

This work was supported in part by the National Natural Science Foundation of China under General Program under Grant 61571468, in part by CPG Research Grant under Grant CPG2017-00028-FST, and in part by the Multi-Year Research from the University of Macau under Grants MYRG2015-00010-FST and MYRG2017-00007-FST.

ABSTRACT A unique method for accurate extraction of coupling coefficient between a lossy radiator and a lossless resonator is proposed in this paper to facilitate the synthesis design of filtering antennas. To remove the parasitic effect of the radiation loss in extraction of coupling coefficient, the network parameters of the coupled resonators in lossless condition is derived and regained from the original lossy network. The unique relationship between the ABCD matrices of the lossless and lossy networks is revealed in detail via their closed-form expressions for both parallel- and series-resonant cases. Next, the coupling coefficient between a rectangular patch antenna and a $\lambda/2$ resonator is numerically extracted with the proposed method, which is further utilized to design a filtering antenna. Finally, the filtering antenna prototype is fabricated and measured, and good agreement among the theoretical, simulated, and measured results has experimentally verified the validity of the proposed method.

INDEX TERMS Coupling coefficient, filtering antenna, accurate extraction, lossy and lossless resonators.

I. INTRODUCTION

With the rapid development of modern wireless communication systems, multiple RF/microwave components have been integrated to achieve a compact size, low cost, and high efficiency of the overall system. As two most essential components at the front end of RF systems, an antenna and filter have been recently designed as a single module, i.e. the so-called filtering antenna, with resorting to the co-design procedure [1]–[3].

Most of the reported filtering antennas can be in general classified into three categories, one kind of which is the antenna connected to the output port of filter as a complex load. Filtering horn and monopole antennas with frequency selective surface (FSS) [4]–[6], filtering patch antenna connected with coupled planar resonator filter [7], [8], and collinear antenna cascaded with substrate integrated waveguide filter have been presented. Another kind of filtering antennas is realized in such a way that metasurface [9], pins and slots [10], and loaded stubs [11] are utilized to introduce radiation nulls to produce filtering gain response. The last kind of filtering antennas is presented and designed according to the traditional filter network, where the antenna is modeled as a lossy resonant GLC circuit to replace the last resonator and the output port of a filter network [12]–[26]. On the one hand, a few of these filtering antennas have been designed with resorting to the equivalent circuit network with J inverters [15]–[18]. On the other hand, plenty of filtering antennas employ external coupled resonators to feed the radiator, and the design procedure requires the prescribed coupling coefficients and external quality factors [21]–[26]. However, to the best of our knowledge, it is very challenging to effectively and accurately extract the coupling coefficient between the lossy radiator and external lossless resonator with the traditional extraction method.

The coupling coefficient was introduced in filter theory and used to tune the filter in the practical design [27], and its measurement method for two symmetrical resonators were present in the early works [28], [29]. Later, for

two symmetrical resonators, the formula of coupling coefficient [30]–[32] is refined with two natural frequencies of the two coupled resonators. The coupling coefficient measurement method has also been extended to the synchronously and asynchronously tuned coupled-resonator circuits, as discussed in [33]. As described above, the coupling coefficient is often extracted from two natural resonant frequencies of two coupled resonators, which are determined by two steep peaks of the transmission coefficient via two weakly coupled external ports. However, it should be noted that this approach is valid only when the two coupled resonators are lossless or when their Q factors are very high. One of the most tremendous distinctions in design between bandpass filters and filtering antennas is that the radiator of a filtering antenna is a lossy resonator with very low unloaded quality factor. For this reason, two steep peaks of the transmission coefficient between the radiators and the external resonators will no longer be observed under weakly coupled excitation. Thus, the desired coupling coefficient between them is unable to be accurately calculated. Thus, an effective method is highly demanded to accomplish this task, i.e., accurate extraction of this coupling coefficient. In recent years, a few works have been reported. In particular, the method in [34] utilizes the amplitude property to evaluate the coupling coefficient between the radiator and external resonator, where only one port coupled to the external resonator is required. Since only the amplitude property at the center frequency is employed, a few parasitic effects, such as shift in resonant frequency of the resonator and dispersive feeding line effect, may result in unexpected errors in the extraction.

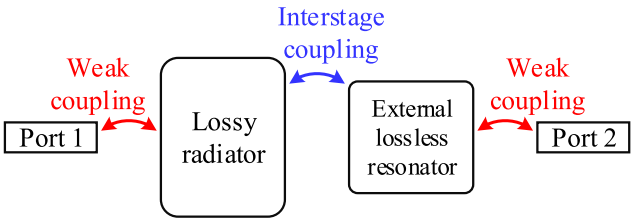

FIGURE 1. Sketch of coupling coefficient extraction between a lossy radiator and an external lossless resonator.

Fig. 1 depicts the sketch of the traditional extraction method of coupling coefficient for filtering antennas, in which the radiator acts as an equivalent lossy resonator. It will be shown latter that two natural resonant frequencies of the interstage-coupled lossy radiator and external lossless resonator will vary with the unloaded quality factor of the radiator, resulting in inaccurate results of coupling coefficient. Moreover, the two peaks of frequency response will be dramatically degraded into one fat peak if the interstage coupling is too weak, which even makes the extraction impossible.

To address this issue, an accurate and general method is proposed in this paper, aiming to regain the lossless network parameters from the original lossy network of the coupled lossy radiator and external resonator. At last, the coupling coefficient between a rectangular patch radiator and a λ/2 resonator is accurately extracted, and the results are then utilized to design a filtering antenna for verification of the proposed method.

II. EXISTING PROBLEMS IN PARAMETRIC EXTRACTION

In this section, theoretical derivation based on circuit model will be conducted to demonstrate why the traditional method for coupling coefficient exaction will lose its validity when the unloaded quality factor of a lossy resonator is very low.

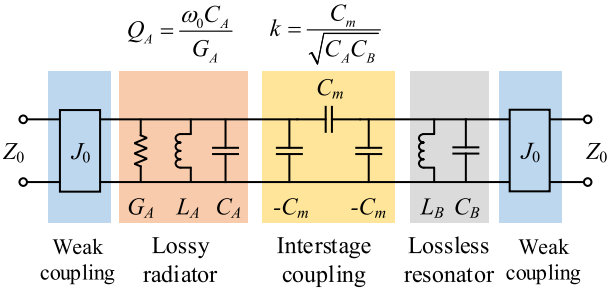

FIGURE 2. The equivalent circuit model of a lossy radiator coupled with a lossless resonator under weakly coupled excitation.

TABLE 1. The circuit parameters in Fig. 2 for demonstration.

Parameters	J_0	f_0	C_A	C_B	Z_0
Values	5×10^{-5} S	4.0 GHz	5 pF	2 pF	50 Ω

Without loss of generality, two resonators under weakly coupled excitation are modeled as the two-port network shown in Fig. 2. Herein, the radiation conductance G_A embodies the loss of the resonant radiator, and its interstage coupling with the lossless resonator is equivalently regarded as a π network of C_m. Besides, the weak coupling between the two resonators and their adjacent ports are represented with J inverters, whose values are very small. As for a typical patch antenna and a half-wavelength micorstrip line resonator, the values of C_A and C_B are set as 5 and 2 pF, respectively, in this example. Part of the circuit parameters are tabulated in Table 1 and the rest will be calculated in the following. The values of L_A and L_B are calculated as

$$L_A = \frac{1}{\omega_0^2 C_A} \tag{1}$$

$$L_B = \frac{1}{\omega_0^2 C_B} \tag{2}$$

where $\omega_0 = 2\pi f_0$.

If the unloaded quality factor (Q_A) and coupling coefficient (k) are specified, G_A and C_m can be obtained with the equations in Fig. 2 as followed

$$G_A = \frac{\omega_0 C_A}{Q_A} \tag{3}$$

$$C_m = k\sqrt{C_A C_B} \tag{4}$$

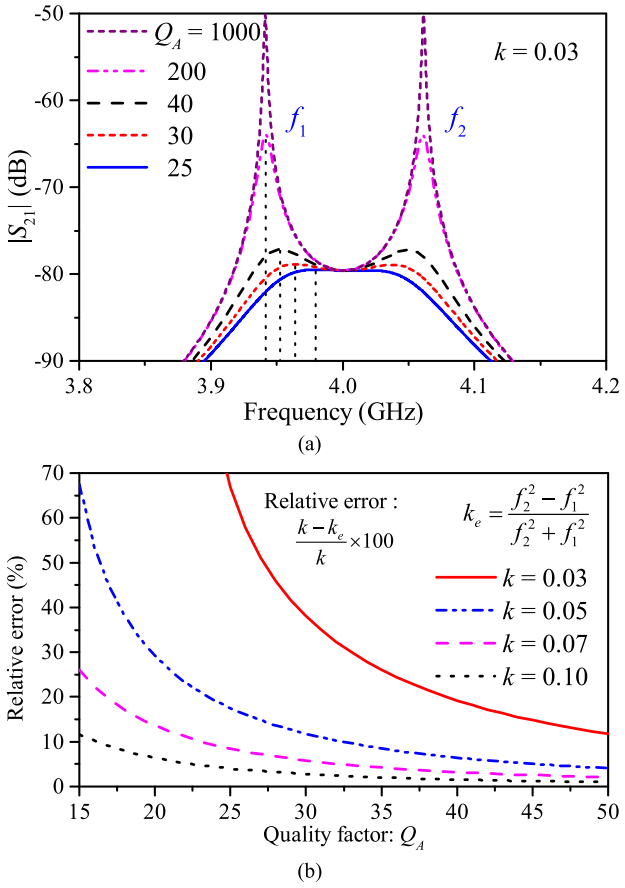

FIGURE 3. (a) The transmission responses under varied Q_1. (b) The relative errors under different Q_1 and k based on the circuit model in Fig. 2.

Till now, all the parameters in Fig. 2 are determined, so that the frequency responses can be now investigated under varied unloaded quality factor (Q_A) and coupling coefficient (k). When k is fixed as 0.03 and Q_A varies from 1000 to 25, the transmission responses are calculated with the results as shown in Fig. 3(a). Herein, two characteristic frequencies, i.e., f_1 and f_2, locate at the two maxima of transmission coefficient. In the reported works [33], the coupling coefficient is derived with these two frequencies, such that

$$k = \frac{1}{2}\left(\frac{f_{02}}{f_{01}} + \frac{f_{01}}{f_{02}}\right)\sqrt{\left(\frac{f_2^2 - f_1^2}{f_2^2 + f_1^2}\right)^2 - \left(\frac{f_{02}^2 - f_{01}^2}{f_{02}^2 + f_{01}^2}\right)^2} \quad (5)$$

where f_{01} and f_{02} are the self-resonant frequencies of each resonator. f_1 and f_2 are the nature frequencies of the two coupled resonators. If f_{01} equals to f_{02}, the coupling coefficient expression of (5) can be simplified as the equation in Fig. 3(b).

As shown in Fig. 3(a), if Q_A is as high as 1000, the radiator can be regarded as a lossless resonator, and two steep peaks appear in the transmission coefficient response, and (5) is accurate in this case. However, as Q_A decreases from 200 to 25, the peaks will be significantly degraded and become more and more flat in shape, and finally only one flat peak emerges. As such, it is difficult or even impossible to determine these two critical characteristic frequencies as inquired in calculation of coupling coefficient.

As illustrated in Fig. 3(a), the characteristic frequency (f_1) under different Q_A is indicated with vertical dashed line. It is evident that f_1 and f_2 tend to gradually increase and decrease, respectively, when Q_A decreases. Please take a special note herein that the coupling coefficient (k) should be only determined by the capacitances C_m, C_A, and C_B, and it has been prescribed with fixed value of 0.03 herein. In other words, k is actually not related to the conductance G_A or the loss at all. However, if the resultant f_1 and f_2 in the case of low Q_A are still employed to extract the coupling coefficient by using (5), the results will become inaccurate and the unexpected error will come up. To be more explicit, the relative errors under varied Q_A and k are calculated. As depicted in Fig. 3(b), the smaller Q_1 and k are, the larger the relative error will be. For example, when k is selected as 0.03, the relative errors for Q_1 equal to 25 and 30 will be raised up to 67% and 38%, respectively, which are definitely unacceptable in design of filtering antenna. Generally speaking, a resonant-type antenna usually has high radiation loss and relatively narrow bandwidth, thus the coupling coefficient and unloaded quality factor are always small. In this context, the coupling coefficient between the lossy radiator and external lossless resonator can not be accurately extracted at all if using the aforementioned traditional method, even though this method is efficient for conventional filter design [33].

III. IMPROVED METHOD

In fact, the flat peaks and parametric extraction error are intrinsically caused by the radiation loss of the patch radiator. If the loss effect of such a radiator is removed, two steep peaks will come up again, such that two natural resonant frequencies corresponding to these two peaks can be then obtained. In the following, the network parameters of the lossless network without radiation loss are at first derived from the ones of its counterpart lossy network. To be more general, both the parallel and series resonant cases will be discussed in the following sections.

A. PARALLEL RESONANT CASE

Fig. 4 depicts the equivalent circuit network, in which the radiator is modeled as an equivalent GLC resonator in parallel with a radiation-caused conductance (G_A). The network in Fig. 4(b) is the lossless counterpart of that in Fig. 4(a), and its coupling coefficient can be accurately extracted with two steep peaks to be known in transmission coefficient response. It should be noted that the two networks have the same interstage coupling and the network parameter in Fig. 4(b) can be derived from that in Fig. 4(a), the accurate coupling coefficient can then be figured out through the given frequency response of the lossy network in Fig. 4(a).

To begin with, the whole circuit network in Fig. 4(a) is divided into three parts, of which the only lossy part,

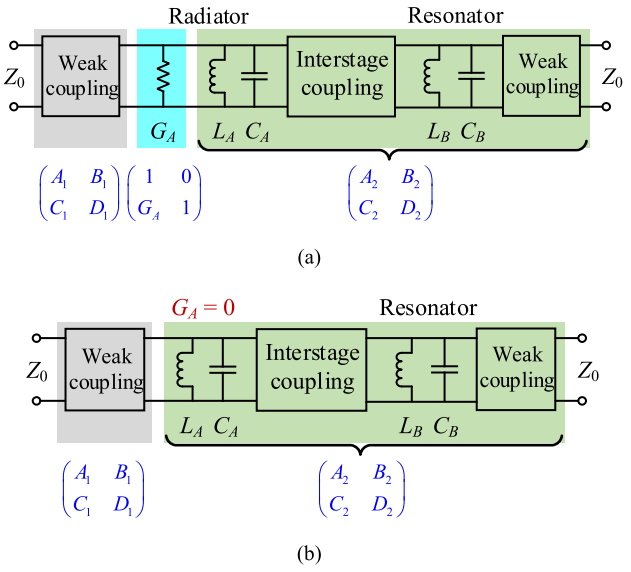

FIGURE 4. Equivalent representation of the coupled radiator and resonator. (a) Lossy radiator with nonzero G_A. (b) Lossless radiator with zero G_A.

i.e., G_A, is solely represented by one matrix. Then the overall response of the network can be derived by multiplying the ABCD matrices of the cascaded parts denoted in Fig. 4(a) and given by

$$\begin{pmatrix} A_p & B_p \\ C_p & D_p \end{pmatrix} = \begin{pmatrix} A_1 & B_1 \\ C_1 & D_1 \end{pmatrix} \cdot \begin{pmatrix} 1 & 0 \\ G_A & 1 \end{pmatrix} \cdot \begin{pmatrix} A_2 & B_2 \\ C_2 & D_2 \end{pmatrix} = \begin{pmatrix} A_1A_2 + B_1C_2 + B_1A_2G_A & A_1B_2 + B_1D_2 + B_1B_2G_A \\ A_2C_1 + C_2D_1 + A_2D_1G_A & B_2C_1 + D_1D_2 + B_2D_1G_A \end{pmatrix} \tag{6}$$

Next, let's consider the lossless counterpart network depicted in Fig. 4(b), where the interstage coupling is kept unchanged but the radiation loss G_A has been excluded. Then the resultant ABCD matrix now becomes

$$\begin{pmatrix} A'_p & B'_p \\ C'_p & D'_p \end{pmatrix} = \begin{pmatrix} A_1 & B_1 \\ C_1 & D_1 \end{pmatrix} \cdot \begin{pmatrix} A_2 & B_2 \\ C_2 & D_2 \end{pmatrix} = \begin{pmatrix} A_1A_2 + B_1C_2 & A_1B_2 + B_1D_2 \\ A_2C_1 + C_2D_1 & B_2C_1 + D_1D_2 \end{pmatrix} \tag{7}$$

Even though the expressions in (6) and (7) look distinctively different, inherent properties of ABCD matrix in (7) make it possible to find a connection between the two networks. For a lossless two-port network, A and D in the ABCD matrix only contain the real part, while B and C only have the imaginary part. Consequently, A_1, D_1, A_2, and D_2 are real, while B_1, C_1, B_2, and C_2 are imaginary, such that

$$A'_p = \mathrm{Re}(A_p) \tag{8a}$$
$$B'_p = j\mathrm{Im}(B_p) \tag{8b}$$
$$C'_p = j\mathrm{Im}(C_p) \tag{8c}$$
$$D'_p = \mathrm{Re}(D_p) \tag{8d}$$

where Re and Im represent the real and imaginary parts of a complex element, respectively.

Then the transmission coefficient of the network excluding G_A could be expressed as

$$S'_{21} = \frac{2}{A'_p + B'_p/Z_0 + C'_pZ_0 + D'_p} = \frac{2}{\mathrm{Re}(A_p) + j\mathrm{Im}(B_p)/Z_0 j\mathrm{Im}(C_p)Z_0 + \mathrm{Re}(D_p)} \tag{9}$$

where Z_0 stands for the port impedance.

Based on (8a)–(8d), the network parameters of the circuit network with zero G_A can be obtained from its original lossy network. After that, the S_{21} magnitude with two steep peaks can be calculated from (9). At last, the two natural resonant frequencies corresponding to the two peaks can be further utilized to calculate the common coupling coefficient of the two networks in Fig. 4 by using with (5).

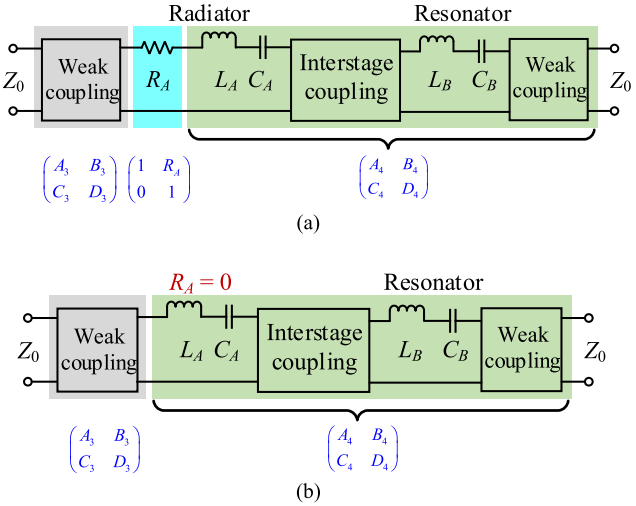

FIGURE 5. An equivalent representation of the series-resonant radiator and resonator. (a) Lossy radiator with non-zero R_A. (b) Lossless radiator with zero R_A.

B. SERIES RESONANT CASE

In addition to the aforementioned parallel resonant case, there is another class of radiators, such as half-wavelength dipoles, which can be modeled as the series RLC resonator. The associated circuit model for coupling coefficient extraction is illustrated in Fig. 5, where a series-resonant lossy resonator is coupled with a lossless resonator. Similarly, the overall ABCD matrix of the whole circuit in Fig. 5(a) can be derived as

$$\begin{pmatrix} A_s & B_s \\ C_s & D_s \end{pmatrix} = \begin{pmatrix} A_3 & B_3 \\ C_3 & D_3 \end{pmatrix} \cdot \begin{pmatrix} 1 & R_A \\ 0 & 1 \end{pmatrix} \cdot \begin{pmatrix} A_4 & B_4 \\ C_4 & D_4 \end{pmatrix} = \begin{pmatrix} A_3A_4 + B_3C_4 + A_3C_4R_A & A_3B_4 + B_3D_4 + A_3D_4R_A \\ A_4C_3 + C_4D_3 + C_3C_4R_A & B_4C_3 + D_3D_4 + C_3D_4R_A \end{pmatrix} \tag{10}$$

Next, the ABCD matrix of the network without R_A or radiation loss in Fig. 5(b) becomes

$$\begin{pmatrix} A'_s & B'_s \\ C'_s & D'_s \end{pmatrix} = \begin{pmatrix} A_3 & B_3 \\ C_3 & D_3 \end{pmatrix} \cdot \begin{pmatrix} A_4 & B_4 \\ C_4 & D_4 \end{pmatrix} = \begin{pmatrix} A_3A_4 + B_3C_4 & A_3B_4 + B_3D_4 \\ A_4C_3 + C_4D_3 & B_4C_3 + D_3D_4 \end{pmatrix} \quad (11)$$

Herein, A_3, D_3, A_4, and D_4 are real, while B_3, C_3, B_4, and C_5 are imaginary. Thus, the following relationship can be obtained

$$A'_s = \mathrm{Re}\,(A_s) \quad (12a)$$
$$B'_s = j\mathrm{Im}\,(B_s) \quad (12b)$$
$$C'_s = j\mathrm{Im}\,(C_s) \quad (12c)$$
$$D'_s = \mathrm{Re}\,(D_s) \quad (12d)$$

It is found that (12a)–(12d) and (8a)–(8d) have the consistent expressions, so the proposed method for coupling coefficient extraction can be applied to both the parallel and series resonant-type radiators in filtering antennas.

C. DISCUSSION

In filter design, there are a few cases in terms of the resonant frequencies of the coupled resonators, which are synchronously and asynchronously tuned. The resonant frequencies of synchronously tuned resonators are the same, while those of asynchronously tuned resonators are different. In the above analysis, there are no requirements on the resonant frequencies of the coupled resonators. Thus, the proposed method is suitable for both types of resonators, showing the advantages of wide applicability.

The proposed extraction method requires two feeding ports, which are weakly coupled to the non-radiative resonator and resonating radiator. For other kinds of filtering antennas, as long as the weakly coupled ports can be added, the proposed extraction method still works. For example, in the design of a waveguide-fed filtering patch antenna, by placing a microstrip feeding in proximity to the patch and a probe weakly coupled to the cavity resonator, the associated coupling coefficient can be extracted with the resultant transmission coefficient.

IV. RESULTS AND VERIFICATION

To examine the effectiveness of the proposed method, the coupling coefficient between a rectangular patch radiator (lossy resonator) and a λ/2 resonator (lossless resonator) in a filtering patch antenna is numerically extracted with this improved technique, and the derived parameter is further utilized to design this filtering antenna.

The geometry of the coupled patch antenna and the λ/2 resonator is shown in Fig. 6, where two weakly coupled feeding lines are placed at two sides. The entire patch filtering antenna is implemented on a Rogers 4003C substrate with a thickness of 1.524 mm and relative permittivity of 3.55. Both the patch radiator and the external resonator are resonating

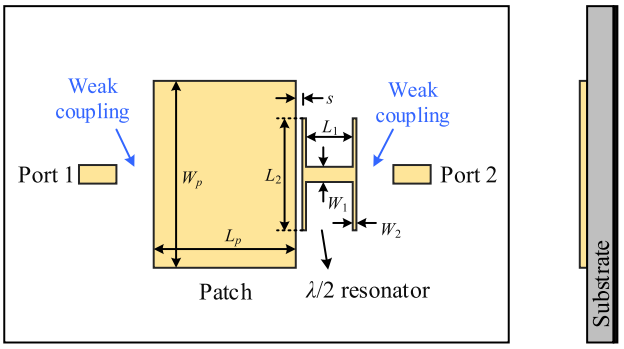

FIGURE 6. The geometry of a rectangular patch radiator coupled with a λ/2 resonator for extraction of coupling coefficient. (a) Top view. (b) Side view.

at 4 GHz, and the dimensional parameters of them are tabulated in Table 2. Because of the symmetrical structure of the λ/2 coupled resonator, TM_{01} mode of the patch radiator will be excited. In the EM simulation, two extra feeding lines are required and weakly coupled to the resonators. In this case, de-embedding is carried out to remove the effects of the feeding lines to ensure the accuracy of coupling coefficient extraction, which can be accomplished in many commercial electromagnetic simulation softwares by moving the reference plane.

TABLE 2. The dimensional parameters.

Parameters	W_p	L_p	L_2	L_1	W_1	W_2
Values (mm)	25	18.5	20	5.63	1.5	0.2

When the gap width (s) between the patch radiator and the λ/2 resonator is selected as 1.5 mm, strong coupling could be achieved to make the peaks in the transmission coefficient response more visible. However, as shown in Fig. 7(a) (dashed line), only two flat bulges appear, resulting in difficulty in determining two characteristic frequencies. It is primarily attributed to the fact that the radiation loss of the patch radiator is high and the Q factor is low accordingly. According to the analysis in the last section, the parameters of the network excluding the loss can be regained by utilizing (8a)–(8d) and (9), and the resulting S_{21} magnitude response is displayed with the solid line in Fig. 7(a). With such post-processing, two steep peaks come up again, which correspond to two natural resonant frequencies of the coupled patch radiator and λ/2 resonator. The characteristic frequencies related to the maxima of $|S_{21}|$ are indicated with vertical lines. It can be clearly figured out that the characteristic frequencies with and without loss effects have considerable distinction between them. Thus, the unexpected error will definitely occur if the characteristic frequencies in the original network corresponding to the two flat peaks are employed in design, as it is demonstrated in Fig. 3.

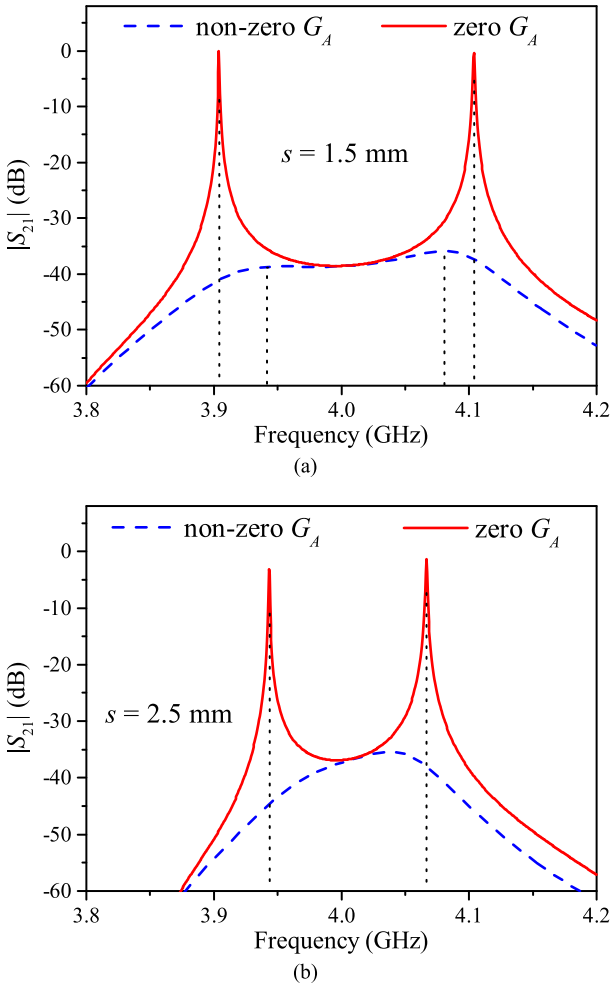

FIGURE 7. Frequency responses of S_{21} magnitudes including and excluding radiation loss for (a) s =1.5 and (b) 2.5 mm.

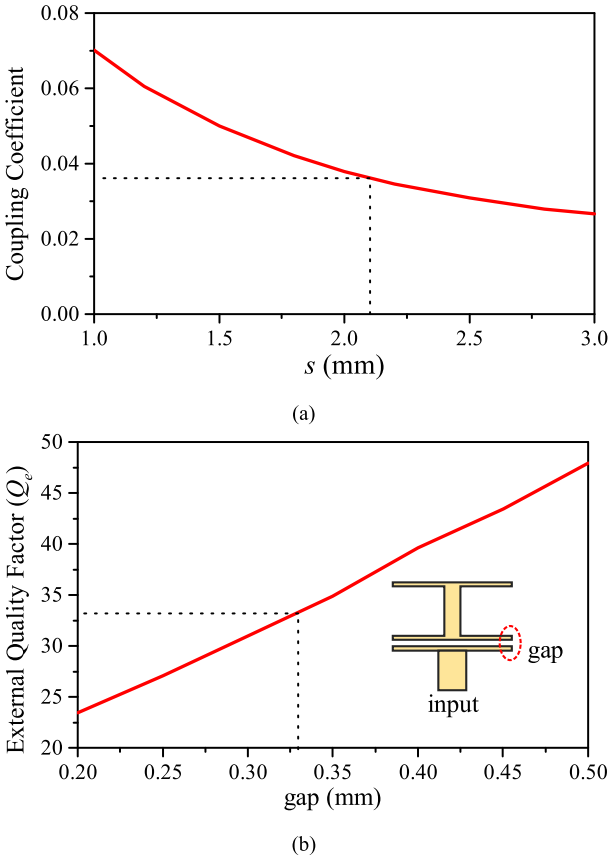

FIGURE 8. (a) The extracted coupling coefficients between the patch radiator and the microstrip-line resonator in Fig. 6 by means of the proposed method. (b) The extracted external quality factor.

When the gap width (s) is selected as 2.5 mm, the interstage coupling will become weaker, and the transmission coefficient response of the original network is displayed with the dashed line in Fig. 7(b). In this case, two natural resonant frequencies of the coupled patch radiator and λ/2 resonator are placed closely to each other, and only one flat peak can be observed because of the radiation loss from the patch radiator. The disappearance of one of two natural resonant frequencies is coincident with Fig. 3(a). Then $|S_{21}|$ of the lossless network is recovered as shown with the solid line in Fig. 7(b). Two steep peaks appear again such that these two frequencies can be found for calculation of the concerned coupling coefficient.

As discussed above, two natural resonant frequencies are obtained from the regained lossless network, and the derived coupling coefficients as a function of the gap distance (s) can be extracted with (5), and the relevant results are plotted in Fig. 8. No matter whether the coupling is strong or weak, it is now always easy to determine the coupling coefficients accurately.

At last, a patch filtering antenna based on the geometry depicted in Fig. 6 is designed with the extracted coupling coefficients. The element values of its corresponding second- order low-pass Chebyshev prototype with the prescribed in-band ripple of 0.2 dB are found as $g_0 = 1$, $g_1 = 1.038$, $g_2 = 0.6746$, and $g_3 = 1.5386$. The dimensions of the patch radiator and the resonator are specified in Table 2, and the unloaded quality factor (Q_A) of the patch can be extracted from simulation, and it turns out to be 32.5 in this work. With two external ports weakly coupled to the patch antenna, the resonant frequency and 3-dB bandwidth are found from the transmission coefficient response to calculate Q_A. Then the theoretical coupling coefficient between the patch radiator and the λ/2 resonator is calculated as 0.038 with the following equations.

$$FBW = \frac{g_0 g_1}{Q_A} \tag{13}$$

$$k_{12} = \frac{FBW}{\sqrt{g_1 g_2}} \tag{14}$$

For the required coupling coefficient of 0.038, the gap width is readily determined as 2.1 mm from Fig. 8. The edge separation between the feeding-line stub and the λ/2 resonator is chosen as 0.33 mm based on the extracted external quality factor. The external Q factor can be extracted with the well-known method described in [33, Ch. 7], where the phase response of reflection coefficient is utilized. As shown

in Fig. 8(b), an input port is added in the feeding line, and then the phase response of S_{11} can be obtained. Suppose that the relative phases at two frequency points, i.e., f_{+90} and f_{-90}, are $+90°$ and $-90°$ with respect to the absolute phase at the resonant frequency f_0, then the external Q factor can be expressed as $Q_e = f_0/(f_{-90}\text{-}f_{+90})$. Because of the port coupling, the resonant frequency of $\lambda/2$ resonator will slightly decrease, and the value of L_1 needs to be slightly adjusted as 5.42 mm to compensate for this effect.

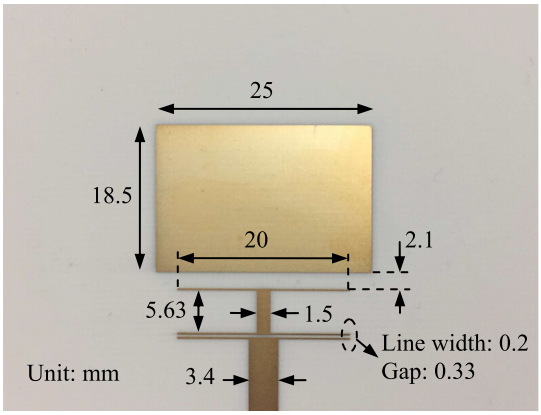

FIGURE 9. The photograph of the fabricated filtering patch antenna.

Fig. 9 shows the photograph of the fabricated patch filtering antenna prototype on the aforementioned dielectric substrate, i.e., Rogers 4003C. The substrate conductivity and dielectric loss tangent are 5.8×10^7 s/m and 0.0027, respectively. Since the theoretical S-parameters are calculated from the ideal circuit model, the simulated result excluding the material loss, e.g., conductive and dielectric losses, are compared with the theoretical ones, while the simulated results including the material losses are compared with the measured ones. The theoretical, simulated, and measured reflection coefficients are all plotted in Fig. 10(a) and (b) for quantitative comparison, and good agreement among them is attained so as to evidently verify the validity of the proposed method. It can be found from Fig. 10(a) and (b) that the simulated reflection coefficient excluding material loss shows larger in-band return loss and better frequency selectivity, and it approximately approaches 0 dB outside the operating band. The simulated result excluding material loss match well with the theoretical one, which verifies the effectiveness of our proposed extraction method. There is a slight discrepancy between the measured result and the simulated one if the material loss is included. This may be caused by a few unexpected factors in practice, such as the discontinuity of SMA connector, uncertainty of dielectric constant, and tolerance in fabrication.

The realized gain of the fabricated filtering antenna is measured with the SATIMO near-field measurement system, and the relevant result is shown in Fig. 11. The gain response seems to be flat around the center frequency with a maximum

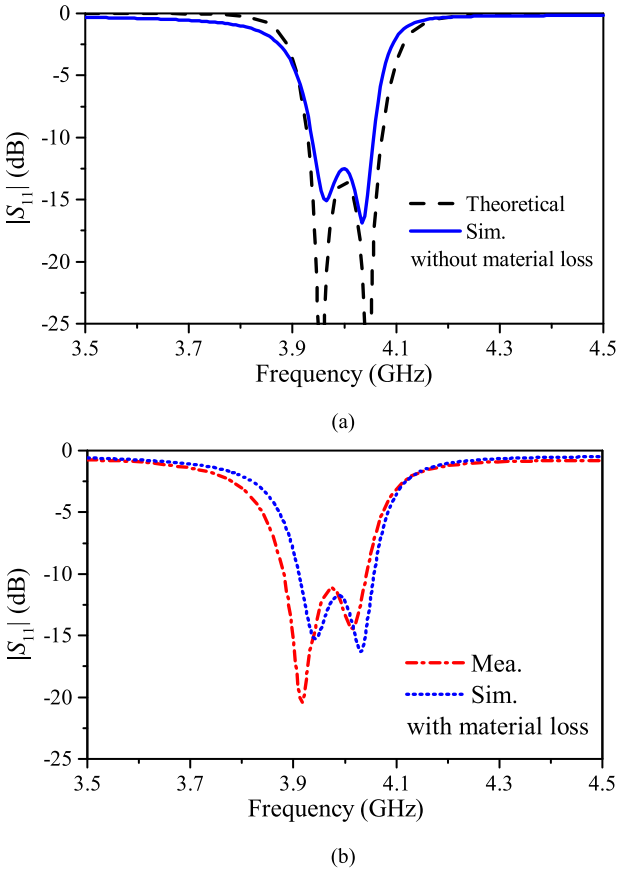

FIGURE 10. (a) Comparison among the simulated reflection coefficient of the antenna in Fig. 9 excluding material loss and the theoretical one. (b) Comparison among the simulated reflection coefficient including material loss and the measured one.

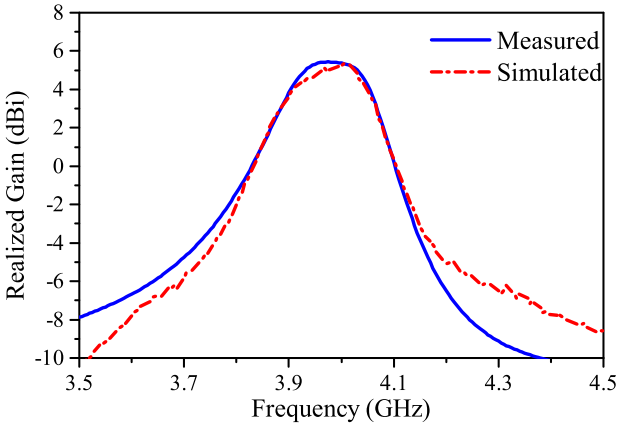

FIGURE 11. The simulated and measured realized gains of the antenna in Fig. 9.

value of 5.3 dBi, whereas its out-of-band counterpart gets significant roll-off, thus showing good filtering characteristics.

V. CONCLUSION

In this paper, an improved method is proposed to accurately extract the coupling coefficient between a lossy radiator and a lossless resonator for synthesis design of the filtering antennas. It is demonstrated that the characteristic frequency

related to the local maxima of transmission coefficient varies with respect to the entire loss of a resonant radiator. At first, notable error has been intensively revealed in calculation of the coupling coefficient if the traditional extracting method is employed. Next, the proposed method is presented to regain the lossless network from its original lossy counterpart via manipulation of ABCD matrix, and the derivation has been described in detail for both parallel- and series-resonant cases. After that, the coupling coefficient between a patch radiator and a $\lambda/2$ resonator has been extracted with the proposed improved method and it is then utilized to design a second-order patch filtering antenna. Finally, the filtering antenna prototype is fabricated and measured, and good agreement among the theoretical, simulated, and measured results has evidently verified the effectiveness of the proposed method.

REFERENCES

[1] T. Le Nadan, J. Coupez, S. Toutain, and C. Person, "Integration of an antenna/filter device, using a multi-layer, multi-technology process," in *Proc. 28th Eur. Microw. Conf.*, 1998, pp. 672–677.

[2] M. Troubat *et al.*, "Mutual synthesis of combined microwave circuits applied to the design of a filter-antenna subsystem," *IEEE Trans. Microw. Theory Techn.*, vol. 55, no. 6, pp. 1182–1189, Jun. 2007.

[3] C.-X. Mao *et al.*, "Integrated dual-band filtering/duplexing antennas," *IEEE Access*, vol. 6, pp. 8403–8411, 2018.

[4] G. Q. Luo *et al.*, "Filtenna consisting of horn antenna and substrate integrated waveguide cavity FSS," *IEEE Trans. Antennas Propag.*, vol. 55, no. 1, pp. 92–98, Jan. 2007.

[5] M. Barbuto, F. Trotta, F. Bilotti, and A. Toscano, "A combined bandpass filter and polarization transformer for horn antennas," *IEEE Antenn. Wireless Propag. Lett.*, vol. 12, pp. 1065–1068, 2013.

[6] H. Zhou *et al.*, "Filter-antenna consisting of conical FSS radome and monopole antenna," *IEEE Trans. Antennas Propag.*, vol. 60, no. 6, pp. 3040–3045, Jun. 2012.

[7] J. Zuo, X. Chen, G. Han, L. Li, and W. Zhang, "An integrated approach to RF antenna-filter co-design," *IEEE Antennas Wireless Propag. Lett.*, vol. 8, pp. 141–144, 2009.

[8] Z. H. Jiang, M. D. Gregory, and D. H. Werner, "Design and experimental investigation of a compact circularly polarized integrated filtering antenna for wearable biotelemetric devices," *IEEE Trans. Biomed. Circuits Syst.*, vol. 10, no. 2, pp. 328–338, Apr. 2016.

[9] Y. M. Pan, P. F. Hu, X. Y. Zhang, and S. Y. Zheng, "A low-profile high-gain and wideband filtering antenna with metasurface," *IEEE Trans. Antennas Propag.*, vol. 64, no. 5, pp. 2010–2016, May 2016.

[10] T. L. Wu, Y. M. Pan, and P. F. Hu, "Wideband omnidirectional slotted patch antenna with filtering response," *IEEE Access*, vol. 5, pp. 26015–26021, 2017.

[11] P. F. Hu, Y. M. Pan, X. Y. Zhang, and S. Y. Zheng, "A compact filtering dielectric resonator antenna with wide bandwidth and high gain," *IEEE Trans. Antennas Propag.*, vol. 64, no. 8, pp. 3645–3651, Aug. 2016.

[12] X. Chen, F. Zhao, L. Yan, and W. Zhang, "A compact filtering antenna with flat gain response within the passband," *IEEE Antennas Wireless Propag. Lett.*, vol. 12, pp. 857–860, 2013.

[13] K. Nadaud, D. L. H. Tong, and E. Fourn, "Filtering slot antenna using coupled line resonator," in *Proc. 9th Eur. Microw. Integr. Circuit Conf.*, 2014, pp. 556–559.

[14] X. Y. Zhang, Y. Zhang, Y.-M. Pan, and W. Duan, "Low-profile dual-band filtering patch antenna and its application to LTE MIMO system," *IEEE Trans. Antennas Propag.*, vol. 65, no. 1, pp. 103–113, Jan. 2017.

[15] C.-T. Chuang and S.-J. Chung, "Synthesis and design of a new printed filtering antenna," *IEEE Trans. Antennas Propag.*, vol. 59, no. 3, pp. 1036–1042, Mar. 2011.

[16] C.-K. Lin and S.-J. Chung, "A filtering microstrip antenna array," *IEEE Trans. Microw. Theory Techn.*, vol. 59, no. 11, pp. 2856–2863, Nov. 2011.

[17] C.-K. Lin and S.-J. Chung, "A compact filtering microstrip antenna with quasi-elliptic broadside antenna gain response," *IEEE Antenna Wireless Propag. Lett.*, vol. 10, pp. 381–384, 2011.

[18] F.-C. Chen, H.-T. Hu, R.-S. Li, Q.-X. Chu, and M. J. Lancaster, "Design of filtering microstrip antenna array with reduced sidelobe level," *IEEE Trans. Antennas Propag.*, vol. 65, no. 2, pp. 903–908, Feb. 2017.

[19] O. A. Nova, J. C. Bohorquez, N. M. Pena, G. E. Bridges, L. Shafai, and C. Shafai, "Filter-antenna module using substrate integrated waveguide cavities," *IEEE Antennas Wireless Propag. Lett.*, vol. 10, pp. 59–62, 2011.

[20] Y. Yusuf and X. Gong, "Compact low-loss integration of high-Q 3-D filters with highly efficient antennas," *IEEE Trans. Microw. Theory Techn.*, vol. 59, no. 4, pp. 857–865, Apr. 2011.

[21] C. Hua, R. Li, Y. Wang, and Y. Lu, "Dual-polarized filtering antenna with printed jerusalem-cross radiator," *IEEE Access*, vol. 6, pp. 9000–9005, 2018.

[22] W.-J. Wu, Y.-Z. Yin, S.-L. Zuo, Z.-Y. Zhang, and J.-J. Xie, "A new compact filter-antenna for modern wireless communication systems," *IEEE Antennas Wireless Propag. Lett.*, vol. 10, pp. 1131–1134, 2011.

[23] M.-C. Tang, Y. Chen, and R. W. Ziolkowski, "Experimentally validated, planar, wideband, electrically small, monopole filtennas based on capacitively loaded loop resonators," *IEEE Trans. Antennas Propag.*, vol. 64, no. 8, pp. 3353–3360, Aug. 2016.

[24] C.-X. Mao, S. Gao, Y. Wang, F. Qin, and Q.-X. Chu, "Multimode resonator-fed dual-polarized antenna array with enhanced bandwidth and selectivity," *IEEE Trans. Antennas Propag.*, vol. 63, no. 12, pp. 5492–5499, Dec. 2015.

[25] C.-X. Mao *et al.*, "An integrated filtering antenna array with high selectivity and harmonics suppression," *IEEE Trans. Microw. Theory Techn.*, vol. 64, no. 6, pp. 1798–1805, Jun. 2016.

[26] H.-T. Hu, F.-C. Chen, J.-F. Qian, and Q.-X. Chu, "A differential filtering microstrip antenna array with intrinsic common-mode rejection," *IEEE Trans. Antenna Propag.*, vol. 65, no. 12, pp. 7361–7365, Dec. 2017.

[27] M. Dishal, "Alignment and adjustment of synchronously tuned multiple-resonant-circuit filters," *Proc. IRE*, vol. 39, no. 11, pp. 1448–1455, Nov. 1951.

[28] S. B. Cohn and J. K. Shimizu, "Strip transmission lines and components: Second quarterly progress report," Stanford Res. Inst., Menlo Park, CA, USA, Tech. Rep. 1114, 1955.

[29] G. L. Matthaei, L. Young, and E. M. T. Jones, *Microwave Filters, Impedance-Matching Networks and Coupling Structures*. Norwood, MA, USA: Artech House, 1980.

[30] K. A. Zaki and C. Chen, "Coupling between hybrid mode dielectric resonators," in *IEEE MTT-S Int. Microw. Symp. Dig.*, May/Jun. 1987, pp. 617–620.

[31] K. A. Zaki, C. Chen, and A. E. Atia, "A new realization of dual mode dielectric resonator filters," in *Proc. 17th Eur. Microw. Conf.*, 1987, pp. 169–174.

[32] A. Abramowicz, "Exact model of coupled dielectric resonators," in *Proc. 20th Eur. Microw. Conf.*, 1990, pp. 1125–1130.

[33] J. Hong and M. Lancaster, *Microstrip Filters for RF/Microwave Applications*. New York, NY, USA: Wiley, 2001.

[34] M. Ohira and Z. Ma, "An efficient design method of microstrip filtering antenna suitable for circuit synthesis theory of microwave bandpass filters," in *Proc. Int. Symp. Antennas Propagat.*, Hobart, TAS, Australia, 2015, pp. 846–849.

QIONG-SEN WU (S'15–M'18) was born in Gaozhou, China. He received the B.Eng. degree in information engineering and the M.Eng. degree in electromagnetism and microwave engineering from the South China University of Technology, Guangzhou, China, in 2011 and 2014, respectively, and the Ph.D. degree in electrical and computer engineering from the University of Macau, Macau, in 2018.

He joined the Antenna and Electromagnetic-Wave Laboratory, University of Macau, Macau, China, as a Research Fellow, in 2018. He is currently an Assistant Professor with the School of Information Engineering, Guangdong University of Technology. His current research interests include microwave circuits and planar antennas with improved functionalities.

XIAO ZHANG (S'15–M'18) was born in Gaozhou, China. He received the B.Eng. degree in information engineering and the M.Eng. degree in communication and information systems from the South China University of Technology, Guangzhou, China, in 2011 and 2014, respectively, and the Ph.D. degree in electrical and computer engineering from the University of Macau, Macau, China, in 2017.

From 2012 to 2014, he was a Research Assistant with Comba Telecom Systems Ltd., Guangzhou, China. He joined the Antenna and Electromagnetic-Wave Laboratory, University of Macau, Macau, China, as a Research Fellow, in 2018. He is currently an Assistant Professor with the College of Information Engineering, Shenzhen University, Shenzhen, China. His research interests include planar antennas and microwave circuits.

LEI ZHU (S'91–M'93–SM'00–F'12) received the B.Eng. and M.Eng. degrees in radio engineering from the Nanjing Institute of Technology (now Southeast University), Nanjing, China, in 1985 and 1988, respectively, and the Ph.D. degree in electronic engineering from the University of Electro-Communications, Tokyo, Japan, in 1993.

From 1993 to 1996, he was a Research Engineer with Matsushita-Kotobuki Electronics Industries Ltd., Tokyo, Japan. From 1996 to 2000, he was a Research Fellow with the École Polytechnique de Montréal, Montreal, QC, Canada. From 2000 to 2013, he was an Associate Professor with the School of Electrical and Electronic Engineering, Nanyang Technological University, Singapore. He joined the Faculty of Science and Technology, University of Macau, Macau, China, as a Full Professor, in 2013, where he has been a Distinguished Professor since 2016. From 2014 to 2017, he served as the Head of the Department of Electrical and Computer Engineering, University of Macau. He has authored or co-authored over 430 papers in international journals and conference proceedings. His papers have been cited over 5400 times with the H-index of 41 (source: ISI Web of Science). His research interests include microwave circuits, guided-wave periodic structures, planar antennas, and computational electromagnetic techniques.

Dr. Zhu served as a member of the IEEE MTT-S Fellow Evaluation Committee (2013–2015) and has been serving as a member of the IEEE AP-S Fellows Committee (2015–2017). He was a recipient of the 1997 Asia–Pacific Microwave Prize Award, the 1996 Silver Award of Excellent Invention from Matsushita-Kotobuki Electronics Industries Ltd., and the 1993 First-Order Achievement Award in Science and Technology from the National Education Committee, China. He served as the General Chair of the 2008 IEEE MTT-S International Microwave Workshop Series on the Art of Miniaturizing RF and Microwave Passive Components, Chengdu, China, and a Technical Program Committee Co-Chair of the 2009 Asia–Pacific Microwave Conference, Singapore. He was the Associate Editor for the IEEE TRANSACTIONS ON MICROWAVE THEORY AND TECHNIQUES (2010–2013) and the IEEE MICROWAVE AND WIRELESS COMPONENTS LETTERS (2006–2012).